River Sediment Fluxes Analysis

In situ measurements and laboratory characterization of cohesive sediment properties (settling velocity, flocculation, hindered settling, consolidation, erosion)

1. Introduction

The physical properties of sediments transported in the Mekong River significantly contribute to the morphological evolution of the delta. At microscopic scale the main processes that ultimately control sediment dynamics are flocculation, floc breakage and hindered settling. Flocculation is the aggregation of primary particles (clay and silt) to form flocs, a phenomenon that is determined by a combination of physical (sediment concentration, turbulence, differential settling) and biological effects. The collision of particles due to different settling velocities is a well-identified process of flocculation (Lick et al., 1993; Hill et al., 1998), yet that has been poorly studied during the last decade.

When fluvial waters enter into the ocean, salinity becomes a driver of flocculation. Flocs breakage is another important process for understanding sediment dynamics. It typically occurs when flocs migrate in regions of highly turbulent conditions. The collision and/or shearing then lead to the disintegration of the most poorly bounded particles. A third important process is hindered settling which is a process that corresponds to the decrease of the settling velocity of flocs when the concentration of particles (by volume) becomes high enough to enhance the fluid viscosity. Flocs are then in strong interactions, which can lead to the stratification of the water column and the presence of lutocline, a sharp density interface which separates the suspended sediment layer on top and the fluid mud layer underneath. Sand particles, which do not flocculate, have a less complex behaviour than flocs as their transport is solely governed by hydraulic laws.

This report focuses on the characterization of the physical properties of suspended sediment in the estuarine area of the Mekong Delta, aiming to quantify the proportion of inert sand and cohesive particles (clay and silt) present in the water column and its change over tidal cycles in the Mekong Delta estuary. More precisely, we aim to characterize the respective influence of suspended sediment concentration, turbulence, and differential settling on the flocculation of particles to provide relevant sediment properties information for the numerical modelling.

This study is based on field surveys and laboratory investigations. We conducted two measurement campaigns during high and low Mekong water discharge in December 2015 and March 2016, respectively, to assess the natural variability of flocs and their dynamics. The laboratory experiments were dedicated to quantifying the respective influence of suspended sediment concentration, turbulence and differential settling on flocculation dynamics. Based on these field measurements and

laboratory experiments, we analyzed the physical properties of the suspended sediment particles and quantified flocculation dynamics.

2. Materials and Methods: Field measurements

Our investigation focuses on the Dinh An channel of the Song Hau distributary, which carries about 30% of the total Mekong River flow to the ocean, making it the largest of the eight channels. Tidal propagation contributes to the mixing of fluvial and oceanic water, and as such, generates important longitudinal and vertical gradients in the water column. During the high flow season, freshwater can extend up to the mouth of the Dinh An, while during the low flow season, salt intrusion has been observed to penetrate up to about 50 kilometres landward of the mouth.

In each survey, we sampled the water from three cross sections (T1, upstream; T2, middle; T3, downstream), separated by distances of 10km and 15km, respectively. The location of the transects was chosen to characterize the saline water intrusion (Fig. 1). Using three Acoustic Doppler Current Profilers (RDI Teledyne ADCP workhorse monitor 600Hz RD Instruments), we measured T1, T2 and T3 simultaneously at hourly intervals for water depth, vertical profiles of the velocity, turbidity and water discharge. We measured the main physico-chemical properties (salinity, temperature and turbidity) of T1 and T3 with two multi-parameter probes (Hydrolab DS5) along three vertical profiles, every two hours along the right bank, centre and left bank during daylight conditions.

For each vertical profile, we obtained SSC (in g/L), Particle Size Distribution (PSD in µm) and calibration of turbidity probes by water sampling. 1 litre of water was collected at the surface, at the bottom of the river, and at 5 metres below the water surface (when water depth was exceeding 7m). The sampling depth was controlled with a pressure sensor, before pumping water with a peristaltic pump. In total, 243 samples were collected at various depths and times (see Table 1). We selected fifteen of those samples, showing contrasted SSC and hydrodynamic conditions, for measuring in situ settling velocity experiments. The limitation to fifteen samples was due to time constraints, as each settling experiment lasts at least five hours.

On March 13th 2016, we also sampled 5 litres of fluid mud near the bottom of transect T3 in order to carry out further analysis in the laboratory

Location	Type of parameter	Instrument	Start date	End date	Number
T1, T2, T3	Flow, velocity	ADCP	10/12/2015 10/03/2016	12/12/2015 13/03/2016	169 181
T1, T3	Temp, depth, salinitiy, turbidity	Hydrolab probe	10/12/2015 10/03/2016	11/12/2015 13/03/2016	37 72
T1, T3	Water sample	Bottles	10/12/2015 10/03/2016	11/12/2015 13/03/2016	74 169

Table. 1. List of the physical quantities measured during field campaigns

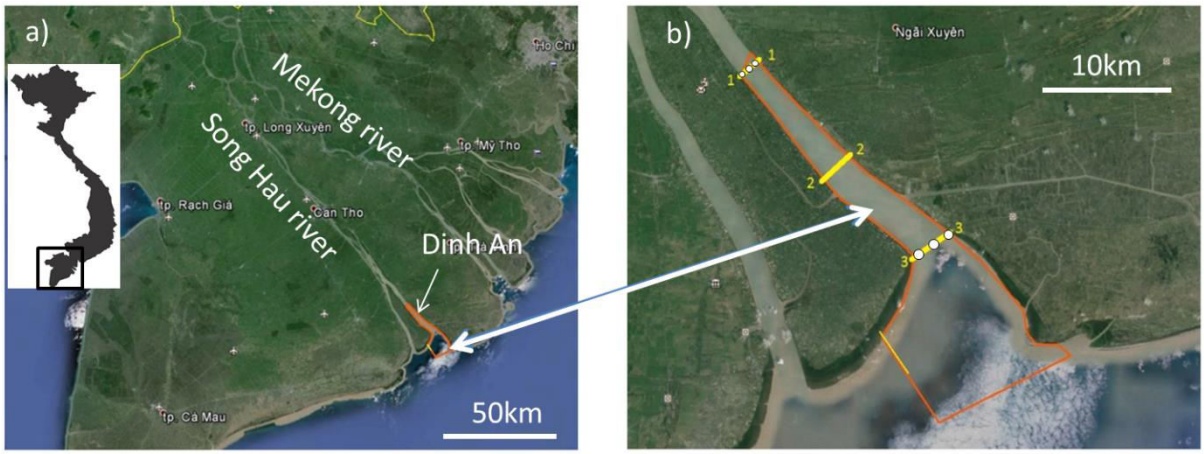

Figure 1: a) Map of the lower Mekong Delta with b) focus on the Song Hau Estuary showing the three transects monitored during the field campaigns

Data processing

We measured SSC on all samples collected. In the present study, all SSC measurements refer to total suspended sediment concentrations (i.e., comprising mineral and organic fractions).

Particle size distribution was measured with a LISST-Portable | XR Sequoia instrument. The typology as in Lee et al. (2014) was used to discriminate individual primary particles of about one micron from the different populations of flocculated particles; namely flocculi of a few microns, micro-flocs of some tens of microns, and macro-flocs of hundreds of microns. The numerical algorithm developed by Launay (2014) was used to separate each population of particles. Based on statistical grounds, a Gaussian law is fitted to each sub-population (calculation of the geometric mean particle size D_f , the corresponding standard deviation σ_{Df} and its relative volumetric concentration. For each sample presented in this study a first measurement was done after sampling and a second measurement was performed after two minutes of sonication (i.e. ultrasound bath). The comparison of the PSDs (Particle-size Distributions) obtained before and after sonication enables a differentiation into the proportion of sand and of flocs, i.e. large particles built by smaller cohesive particles (silt or clay), which are destroyed by the sonication. The salinity of the sample used for lab experiments was 17.

The design of the experimental set-up was based on the conceptual diagram of Dyer (1989) reproduced in Figure 2. This diagram establishes a relationship between the mean turbulent energy dissipation rate G (in s^{-1}), the suspended sediment concentration (SSC in g/L) and the mean floc diameter D_f (in µm). As depicted in this figure, the mean floc size of a population (blue curvative surface in Fig. 2) results from a dynamic equilibrium between floc breakage by collision or internal shearing (Kranenburg, 1994; Gratiot and Manning, 2004) and flocculation. In Dyer's diagram (1989), D_f can vary over more than one order of magnitude for different concentrations and levels of turbulence. For high turbulence levels above 20-50 s^{-1}, Dyer's diagram predicts a predominance of floc breakage, so that the size of aggregated particles does not exceed a few microns. Optimal conditions of flocculation are expected to occur under quiescent conditions or gentle turbulence (a few s^{-1}) and for suspended sediment concentration as high as SSC=10 g/L

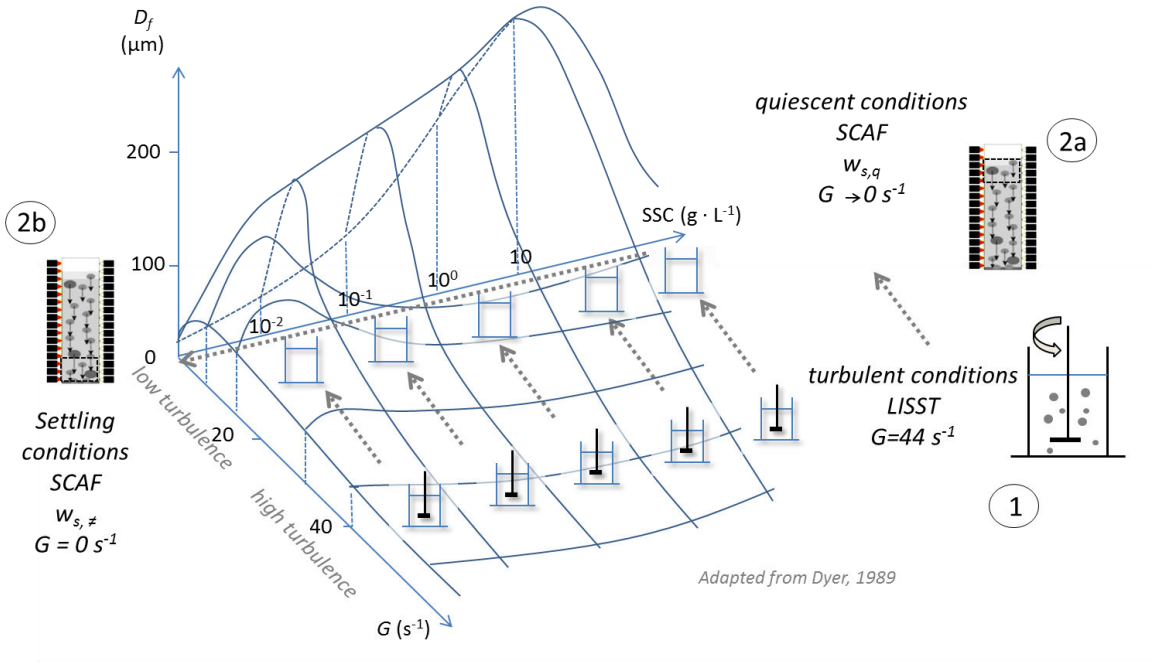

Figure 2. Experimental procedures superimposed on the conceptual diagram of Dyer (1989). Experiments are first conducted in a jar tank under turbulent dominated conditions (step 1) and secondly in SCAF (System for the Characterisation of Agregates and Flocs; Gratiot et al., 2015) system under settling dominated conditions (step 2a and 2b)

The laboratory investigations consisted of three steps aiming at characterising turbulence, quiescent and settling dominated conditions. The strategy was to cover a wide range of situations in Dyer's diagram with a reasonable number of runs. In total, 21 experiment runs were performed for SSC values covering a wide range, from free settling regime (SSC=0.02 g/L, no interactions between particles during their settling) to hindered regime (SSC =99.0 g/L, strong interactions between particles which hinder their settling).

For each run, a volume of 2 litres of water sediment mixture was introduced into the tank and mixed with an impeller for thirty minutes. This duration can be too short to reach the equilibrium regime between flocculation and deflocculation (Tran and Strom, 2017), but is believed to be representative of the maximum duration with nearly constant turbulent conditions in tidal flows. The rotation of the impeller was fixed at 100 rpm, which corresponded to a mean turbulent energy dissipation parameter G of 44 s^{-1}.

After measurements were taken under turbulent conditions, 160 mL of fluid-sediment mixture was pumped from the jar tank and placed in the SCAF settling tube to characterize flocculation under quiescent and settling conditions. The SCAF settling tube is an optical settling column, equipped with a vertical array of sixteen optical sensors (Gratiot et al., 2015). In the SCAF instrument, some detailed characteristics of floc settling velocities are deduced from the decrease of turbidity over time (Wendling et al., 2015; Mercier et al., 2016). Measurements taken in the upper part of the SCAF settling tube during the first minutes provided an estimation of flocs settling velocity under quiescent conditions $w_{s,q}$ (step 2a), while measures realized near the bottom of the settling tube after several

tens of minutes provided an estimation of flocs settling velocity by differential settling under settling dominated conditions $w_{s,\neq}$ (step 2b).

3. Results

a. Stratification of the water column and high suspended sediment concentration near the river bottom

Figures 3a and 3b show vertical profiles of temperature (blue circles), salinity (blue dots) and SSC (black crosses) recorded on the right bank of the river at transects T1 and T3 during high tide on the 11th and 10th of December 2015 at 17:07 and 17:30 local time, respectively. It typically illustrates the vertical distribution of suspended sediment and stratification of the water column. Similar profiles were observed many times at both transects T1 and T3 during the two field surveys. The vertical profile of SSC shows a marked stratification, with jumps in SSC (called lutocline) and salinity (called halocline) in the water column. These stratifications are lutoclines of which two (or three in Fig. 3b) can be observed.

This simultaneous evolution between SSC and salinity, observed in both transects, indicates that the lutocline is associated with the tidal-induced movement of the salt wedge in the estuary. It means that SSC dynamics is influenced by hydrodynamics (the change in flow) and the associated dynamics of salinity. There is no thermocline, as water temperature ranges from 30.3°C near the surface to 30.15°C in the concentrated layer.

Although much larger SSC values were not recorded due to instrumental and practical constraints (the sensor of the probe does not reach the riverbed because of the protective cage and reaches saturation at 3000 NTU (which corresponds to 4.4 g/L), it can be expected that they reach tens or even hundreds of grams per litre, as observed in other muddy estuarine systems (Mehta, 1989; Winterwerp, 2002; Sottolichio et al., 2011). This near bed lutocline is not associated with a halocline or a thermocline.

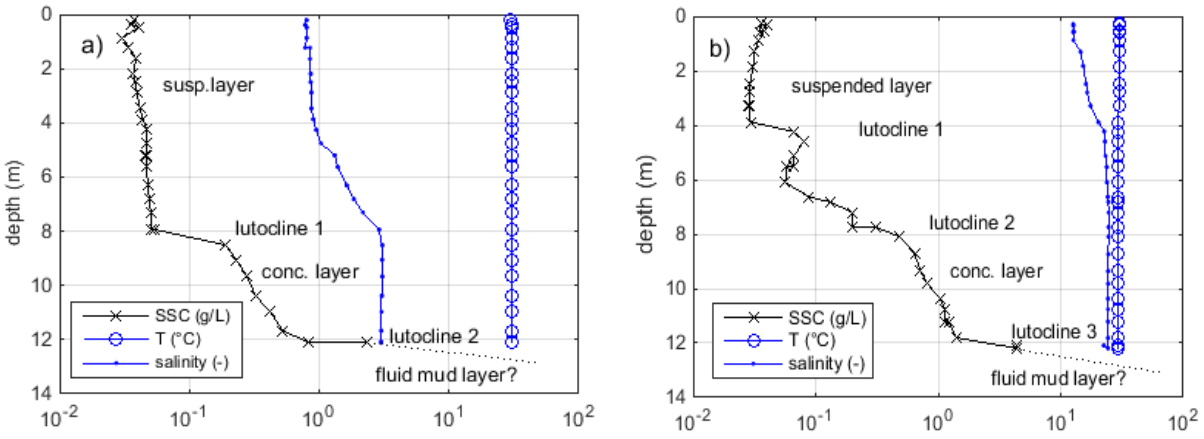

Figure 3. Vertical stratification of the water column measured at a) transect T1 on the 11th of December 2015 at 17:30 local time. b) transect T3 on the 10th of December 2015 at 17:07 local time

b. Influence of SSC on floc dynamics under turbulent dominated conditions

Typical PSDs measured in the experiments under turbulent conditions for low (SSC~20 mg/L), high (SSC~800 mg/L) and very high (SSC~2,000 mg/L) concentrations are shown in Figure 4 and illustrate the impact of increasing concentration on flocculation: at low concentration, the PSD exhibits a unimodal distribution (on a logarithmic scale) with a population of particles between 1.0 to 100 µm and a median of 9.6 (±1) µm. Conversely, at high concentration the PSD shows a bimodal distribution (on a logarithmic scale). The finest population displays a similar distribution to that observed at low concentration with particles between 1 to 100 µm and a median of 12 (±2) µm. A second population develops for particles coarser than 100 µm. This second population has a median of 211 (±30) µm. The population of small particles predominates and corresponds to 90% of the total volume of particles (Fig. 4b). At very high concentration, the PSD obtained is broadly similar to that obtained at high concentration (Fig. 4c). The fine population has a median of 10.1 µm, while the median of the second population is 151 (±25) µm. As for the high concentration, the volumetric concentration of the small population also dominates (84% of the total volume).

Figures 4e and 4f show the PSD of the same samples after two minutes of sonication. The time gap between the end of sonication and measurements is about 5 seconds. The sonication broke the flocs, revealing the PSD of the elementary particles. In both cases, the larger particles disappeared, indicating the breakup of the large flocs. By replacing the original large flocs, three populations of particles are identified: one that was in the range of the first population before sonication, one smaller, and one slightly larger than this central population. Similar results were obtained for all laboratory samples with high SSC.

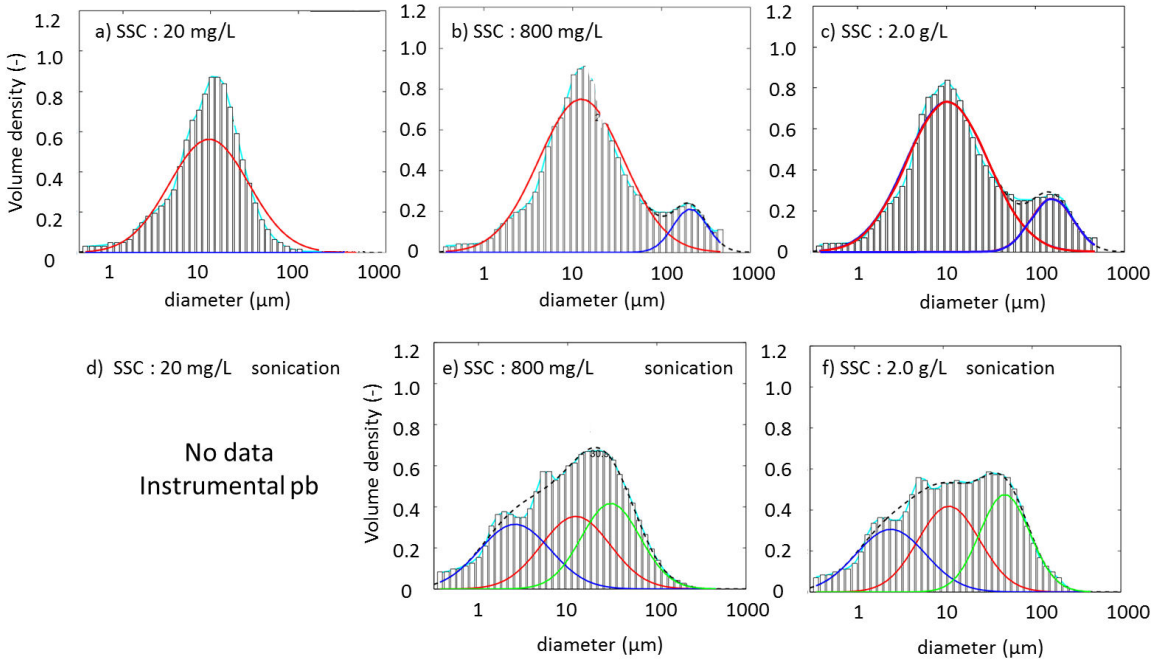

Figure 4. Particle Size Distributions (PSD) of particles sampled during the jar tank experiment for low, high and very high SSC. These PSDs were obtained before sonication (4a, 4b, 4c) and after sonication (4e, 4f). Due to instrumental limitation (very low SSC), no data was acquired after sonication at 20 mg/L with LISST system. Red, blue and green curves corresponds to the numerically identified sub-populations

Figure 5 shows the principal characteristics of floc populations for both laboratory (left panels) and field (right panels) measurements. The variation of PSD with concentration, as measured in the field (Fig. 5b and 5d), shows the same flocculation characteristics as seen in the laboratory experiments (Fig.5a). In particular, the existence of a unimodal distribution can be observed for SSC values lower than 200 mg/L, a transition zone between 200 and 500 mg/L, where unimodal and bimodal distributions coexist, and bimodal distributions for higher concentrations. We note that the size of macro-flocs and flocculi do not increase with SSC. From Figure 5, it can be seen that results from field and laboratory experiments are in agreement and that flocculi is the dominant particle population (80-100%). It is also interesting to note that the particle size is slightly larger for the field samples (geometric mean D_p = 15 µm) than for the laboratory samples (geometric mean Dp = 10 µm); this point is examined in the discussion section.

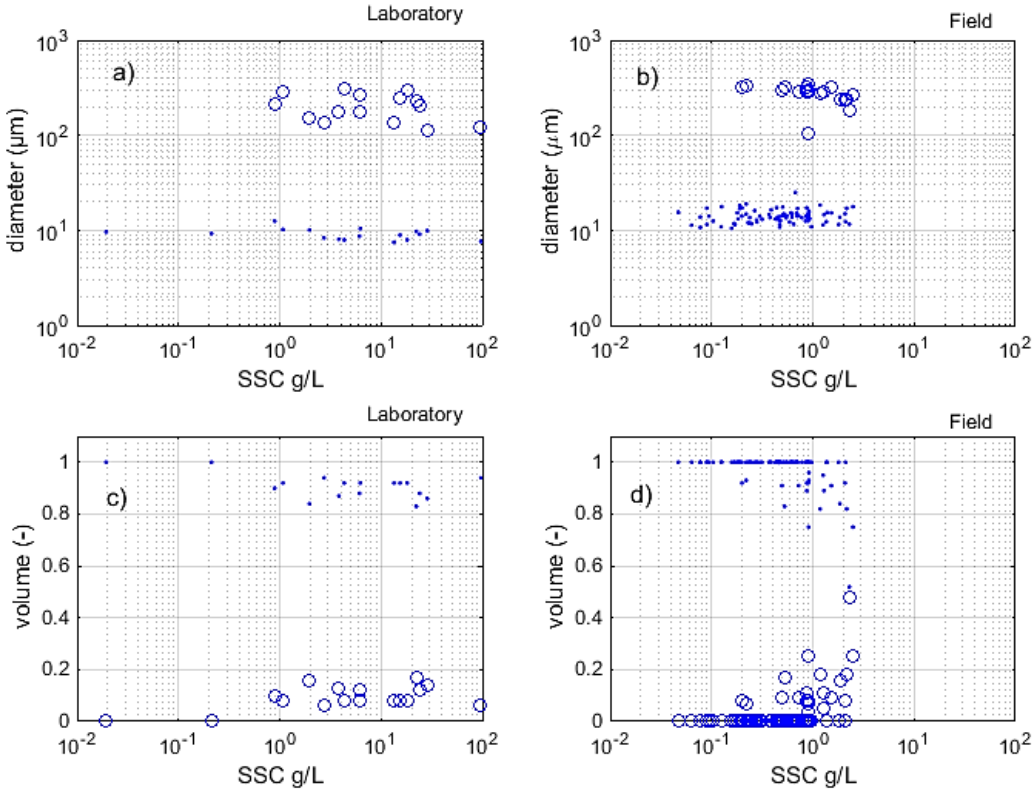

Figure 5. Intercomparison between particle size and floc characteristics for laboratory (6a and 6c) and field (6b and 6d) samples under turbulent dominated conditions. a and b: Variation of mean particle diameter with SSC. If for the same SSC a circle and a dot is shown, two sub-populations of particle sizes exist (bimodal particle size distribution); c and d: Variation of the volumetric partition between flocculi (dots) and macro-flocs (circles) for increasing SSC values

c. Influence of SSC on floc dynamics under quiescent and settling dominated conditions

Sedimentation for low (SSC ~ 20 mg L-1), high (SSC ~ 800 mg L-1) and very high (SSC ~ 2,000 mg L-1) concentrations is reported in Figure 6. These graphs show the decrease of turbidity in the settling column over time and space. Complete sedimentation required about four hours for the run

performed at low concentration (Fig. 6a) and less than one hour for runs conducted at high and very high concentrations (Fig. 6b and 6c).

Sedimentation of particles in the SCAF settling tube provides two different settling velocities: ws,q corresponds to the velocity when particles are settling in a fluid at rest (quiescent conditions) ; ws, ≠ , corresponds to the increased velocity when particles have been flocculating together by differential settling. In Figure 6, ws,q is about 1.1 10-5 m/s for a SSC value of ~ 19 mg/L . It increases by an order of magnitude to 1.0 10-4 m/s for high concentrations (SSC ~ 800 mg· L-1), and shows an additional 40% increase for very high concentrations (SSC ~ 2000 mg/L for which ws,q =1.4 10-4 m s-1). The settling velocity ws, ≠ measured near bottom reaches values of 4.0 10-5 m s-1, 2.5 10-4 m s-1 and 1.0 10-3 m s-1 , for the same SSC values of ~19, ~800 and ~2000 mg/L (i.e. a respective 3.6, 2.5 and 7.1 fold increase of the settling velocity caused by the flocculation by differential settling). As a preliminary conclusion, results presented in Figure 6 show that with increasing SSC, the settling velocity also increased as a result of flocculation.

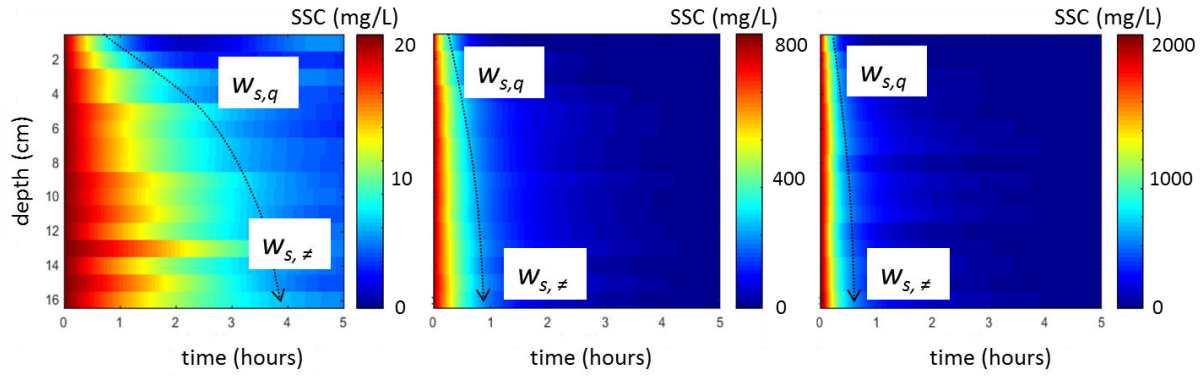

Figure 6. Variation of SSC with time during the settling of particles measured by the SCAF instrument for low, high and very high SSC conditions

Figure 7a compares field and laboratory measurements. Both show similar patterns but the field data are more dispersed. For suspended concentrations below 300 mg/L the settling velocity is constant for both quiescent and differential settling regimes. For higher concentrations, settling velocity increases because of the flocculation of particles. The maximum settling velocity is obtained for the highest suspended sediment concentration sampled (SSC=2.4 ± 0.2 g/L) and reaches a value as high as ws,q ~4.5 10-4 m/s and ws, ≠ ~2.8 10-3 m/s. Flocs settling velocity estimated in the field were systematically higher than the ones obtained in the laboratory. Furthermore, under field conditions, it was not possible to explore the hindered regime because of technical limitations for sampling. The highest SSC values are observed in a thin layer near the riverbed, which cannot be sampled in the field (see Fig. 3).

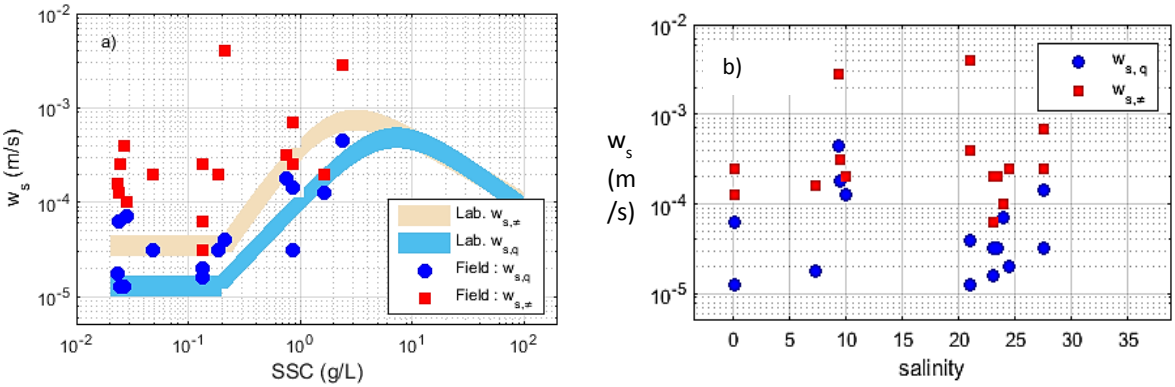

Figure 7. Variation of the settling velocity of particles with suspended sediment concentration: Squares and circles correspond to settling velocity under quiescent and settling conditions in the field, respectively. Grey lines correspond to the laboratory experiments.b) Effect of salinity on settling velocity of particles in the field

Figure 7b investigates whether salinity affects the settling velocity in the field measurements. Contrary to the laboratory experiments, where the salinity was fixed (S=17), salinity during the field measurements varied markedly along the vertical and longitudinal direction (see Fig.3a and 3b), but also with tidal cycle. However, Figure 8d does not show any clear relation between salinity and settling velocity, which differs from the observations of Kumar et al. (2010). This may be due to an important co-variation of salinity with other hydrodynamic and biogeochemical factors during the tidal cycle. For example, the intrusion of saline water during floods also coincides with resuspension of sediments from the riverbed and high levels of turbulence. Salinity, sediment concentration and turbulence are three drivers of flocculation and deflocculation that vary simultaneously, so that their respective effects can barely be identified from field measurements. However, it can be hypothesized that the different salinity levels are at least partly responsible for the spread of the settling velocities for the field samples shown in Figure 7a, particularly at low SSC.

4. Discussion and conclusions

Our first objective to characterize whether particles transported in the water column were inert (sand) or cohesive (clay, flocculi and flocs). For the whole set of suspended sediment samples collected during two field campaigns in the high and low flow season (243 samples), we found that cohesive sediment was predominant. Analysis of the particle size distributions at no point showed the existence of sand in suspension. This was demonstrated by PSD measurements before and after sonication, which destroys any flocs present in the samples. While some samples had PSDs with sub-populations peaking around 120-300 µm, i.e. in the range of sand particles, all of them were transformed by sonication into smaller particles. This indicates that sand is not present in suspension in the Mekong estuary. However, it must be noted that sand was occasionally found in bottom sediment samples from the riverbed, indicating the presence of sand on the riverbed (ws~260 microns, Dp ~3.310-2 m.s-1).

Our second objective was to characterize the respective impacts of sediment concentration and turbulence level on the flocculation process. The major results we obtained are as follow:

PSDs systematically exhibited a unimodal population of flocculi for sediment concentrations below 200-300 mg/L in turbulent conditions. For higher concentrations, the flocculation process led to the formation of macro-flocs with diameters in the range of 150≤ Dp ≤300 µm, i.e. fifteen times larger than the mean diameter of the flocculi population (8.0≤ Dp ≤20.0 µm). These macro-flocs contribute to a significant increase of sediment settling flux because of their large size, even if they account for less than 20% of the total sediment volume (Fig. 5c and 5d).

The examination of field and laboratory data shows that flocculation was found to be systematically higher in situ than in the laboratory (Fig. 5 and Fig. 7). A first explanation might relate to the experimental device. It is believed that the high level of turbulence (G~44 s-1) required to maintain the largest flocs in suspension in the jar tank may have limited their growth, inertial forces of eddies overpassing binding forces, as described by Kranenburg (1994). Another hypothesis might relate to the nature of the particles. Estuarine areas are known to be catalyzers of biogeochemical processes, and biological activity often has an important effect on floc dynamics (Verney et al. 2009; Mari et al., 2012). We cannot exclude that storage conditions in the dark tank at 6°C during transportation into the laboratory had altered the organic matter and reduced its ability to flocculate. Despite this slight difference between floc properties in the field and in the laboratory, experimental conditions offered the possibility to explore a wider range of concentrations (from 20 mg/L to 99,000 mg/L) and regimes (free, flocculated, hindered) than in the field.

A global comparison of our experiments with those in the literature is presented in Figure 8. This figure shows the reactive nature of flocculation in the natural Mekong River estuarine fluid mud determined in this study compared to a large range of other mud settings (synthesized in Table 2). Before comparing the data, it must be kept in mind that the various techniques used in prior studies can generate inherently different results (along the Y axis), as suggested by Ross (1988). Furthermore, most prior experiments focused on the flocculation regime (experiments 1 to 18) and only five studies covered the full range of settling regimes, up to the hindered regime (experiments 19 to 23). However, the comparison shows that the floc characteristics of the Mekong Estuary (present study, n°23, circles) have several specificities.

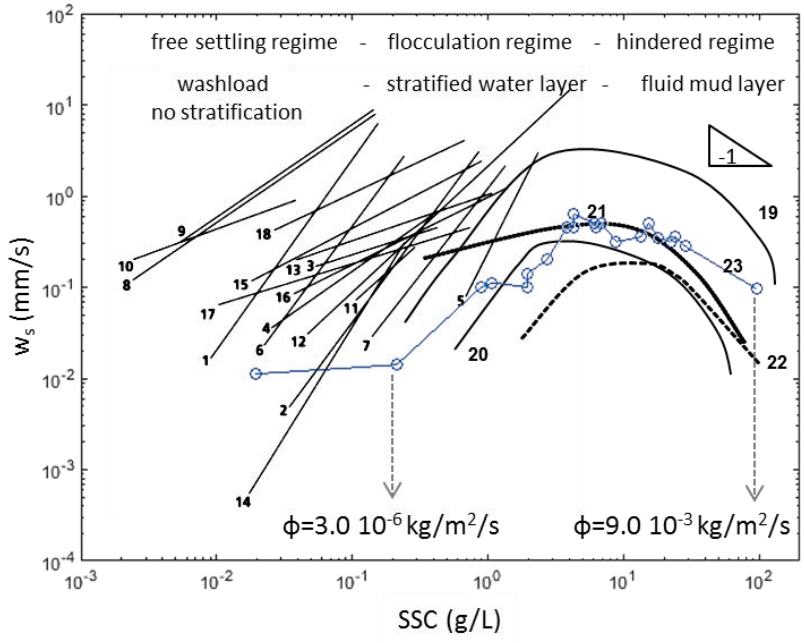

Figure 9. Regression curves showing the variation of settling velocity with suspended sediment concentrations obtained by various authors from field experiments for a range of temperate estuaries and bays (adapted and completed from Pejrup and Mikkelsen (2010) and Gratiot and Anthony (2016)), and from the Mekong river mouth (circles, present study). The various sites are referenced in Table 3

Site number and author(s)	Location and years of sampling	Country	Instrument
1/2 Puls et al. (1988)	River Elbe 1985–1986	Germany	Braystoke tube
3/4 Puls et al. (1988)	River Weser 1985	Germany	Braystoke tube
	River Tamar		
5/6/7 Barton et al. (1991)	1986-1987-1988	United Kingdom	Owen tube
8/9/10 Edelvang and Larsen (1995)	Ho Bay 1989-1990	Danish Wadden Sea	Braystoke tube
11 Andersen (1999)	Rømø Bay 1997	Danish Wadden Sea	Braystoke tube
12 Burt (1986)	River Thames 1969–1983	England	Owen tube
13 Pejrup (1988)	Ho Bay and Rømø Bay 1983–1984	Danish Wadden Sea	Braystoke tube
14 Jones and Jago (1996)	River Elbe 1993	Germany	QUISSET tube
15 Pejrup and Edelvang (1996)			Braystoke tube
16/17/18 Dyer et al. (1996)	River Elbe 1993	Germany	Owen tube
19 Thorn (1981)	Severn Estuary	UK	

20 Ross (1988)	Tampa bay	USA	Settling column, by SSC sampling
21 Sottolichio et al., (2011)	Gironde estuary 2007	France	Bergen Nautik Sedimeter
22 Gratiot and Anthony (2016)	Kaw river mouth, 2001	French Guiana	Settling column, Bergen Nautik Sedimeter
23 present study	Song Hau river mouth, 2015-2016	Vietnam	SCAF settling tube

Table 3. *Sites and references for flocculation and settling velocity comparisons shown in Fig.9.*

For SSC≤200 mg/L, the characteristics of flocculi in the Mekong River are not influenced by sediment concentration; the settling velocity seems to remain constant, which is unique for the 23 available datasets (Fig. 9). Comparably, the settling velocities in the Mekong estuary were relatively low, which may be attributed to the characteristics of their flocs and the signature of the upstream fluvial environment. The existence of this free settling regime implies that **floc characteristics in the water column can be adequately modelled with a single class of flocculi particles** (Df in the range 8-20 µm and ws in the range 1-8 10-5 m/s) as long as SSC≤200 mg/L. Because settling velocity is very low for this range of concentration (1-2 10-5 m/s), we may expect a fairly homogeneous distribution of SSC over the water column (washload regime with no stratification).

For 200 mg/L < SSC < 2-6 g/L, settling velocity increases quite linearly with SSC (power coefficient 1.25<<1.7 in Table 2). The modification of floc characteristics in this range of concentration is similar to that observed in other rivers and estuaries worldwide.

For SSC> 2-6 g/L, the settling velocity decreases with SSC, which is characteristic of the hindered regime. This decrease is rather gentle with the direct consequence being that sediment settling flux ϕ=ws x SSC increases even for concentrations up to SSC=99.0 g/L. Sediment settling flux starts to decrease for SSC values beyond 30 g/L for all other rivers and estuarine environments reported in Figure 8.

At the scale of the Mekong Delta, particles are expected to be mainly transported as washload within the river flow. Inland SSC rarely exceeds a few tens of milligrams per liter, which corresponds to the free settling regime with low settling velocity. Upon their arrival into the delta distributary mouths, the combined effects of the saline gradient and the tidal mixing of fluvial and oceanic waters enhance flocculation and induce water stratification (Fig. 3). **Along the surrounding creek and mangrove fringes, the lower turbulence conditions offer favourable conditions to initiate flocculation by differential settling. Then, sediments will be most likely trapped locally because Mekong sediment settling flux ϕ is very high.** When compared to the other two tropical environments with available data (Tampa bay, Florida, n°20 and Kaw river mouth, French Guiana, n°22, in Fig. 8), sediment settling flux ϕ is at least one order of magnitude higher for SSC > 100 g/L.

The assumption of a local trapping in the delta distributary mouths region of the Mekong Estuary is sustained by the observed geomorphic changes described by Anthony et al. (2015, Fig. 3 of their paper). Based on a satellite survey of shoreline changes, they observed that the bed load sediment transport and deposition in the delta distributary mouths is in balance with erosion, while the coastal regions of the Mekong Delta located further away from the river mouths has been eroding at an unprecedented mean rate of 20-25 m/y. In forthcoming decades, we may expect that flocs

properties ensure the trapping of sediment in river mouths and that erosion will pursue in the coastal regions.

Acknowledgments: This work has been conducted as part of a broader collaboration. A.Bildstein, H.Denis, H.Michallet, J.Némery and T.Phong are fully acknowledged for their kind help during the laboratory experiments; we also would like to acknowledge all colleagues involved in the field survey, in particular, T.T. Anh, H.Thoss and H.Apel, as well as colleagues from SIWRR. This project was mainly funded by LMDCZ project, and partially funded by Institut de Recherche pour le Développement, GFZ German Research Centre for Geoscience, as well as ANR SCAF JCJC ANR-12-JS06-0006 project. Scholarship funding by the German Academic Exchange Service DAAD (NAWAM programme, Nr. 91587027) of the PhD work of Tran Tuan Anh is gratefully acknowledged

REFERENCES

Andersen, T.J., 1999. Suspended sediment transport and sediment reworking at an intertidal mudflat, the DanishWadden Sea. Meddelelser fra Skalling-Laboratoriet 37 Institute of Geography, University of Copenhagen.

Anthony, E. J., Brunier, G., Besset, M., Goichot, M., Dussouillez, P. and Nguyen V.L. 2015. Linking rapid erosion of the Mekong River delta to human activities. Sci. Rep. 5, 14745; (2015).

Barton, M.L., Stephens, J.A., Uncles, R.J., West, J.R., 1991. In: Elliott, M., Ducrotoy, J.P. (Eds.), Particle fall velocities and related variables in the Tamar Estuary. Estuaries and Coasts: Spatial and Temporal Intercomparisons. Olsen & Olsen, 31–36.

Burt, T.N., 1986. Field settling velocities of estuary muds. In: Mehta, A.J. (Ed.), Estuarine Cohesive Sediment Dynamics. Lecture Notes on Coastal and Estuarine Studies vol. 14. Springer-Verlag, 126–150.

Dyer, K.R., 1989. Sediment processes in estuaries: future research requirements. J. Geophys. Res. 94 C10 , 14327–14339.

Dyer, K.R., Cornelisse, J., Dearnaley, M.P., Fennessy, M.J., Jones, S.E., Kappenberg, J., McCave, I.N., Pejrup, M., Puls, W., van Leussen, W., Wolfstein, K., 1996. A comparison of in situ techniques for estuarine floc settling velocity measurements. J. Sea Res. 36, 15–29.

Edelvang, K., Larsen, M., 1995. The flocculation of fine-grained sediment in Ho Bugt, the Danish Wadden Sea. Folia Geographica Danica. Reitzels Forlag (TOM XXII.C.A.).

Gratiot, N. and Anthony, E.J. 2016. Role of flocculation and settling processes in development of the mangrove-colonized, Amazon-influenced mud-bank coast of South America. Mar. Geol., 373, 1-10.

Gratiot, N., Coulaud, C., Legout, C., Mercier, B., Mora, H.Wendling, V., 2015. Unit for measuring the falling speed of particles in suspension in a fluid and device comprising at least one measuring unit and one automatic sampler. Patent-Publication number WO2015055963 A1

Gratiot, N. and Manning, A.J 2004. An experimental investigation of floc's characteristics in a diffusive turbulent flow. Journal of Coastal Research, SI(41), 105-113.

Hill, P. S., Syvitski, J. P., Cowan, E. A., and Powell, R. D. (1998). In situ observations of floc settling velocities. Marine Geology, 145:85–94.

Jones, S.E., Jago, C.F., 1996. Determination of settling velocity in the Elbe estuary using QUISSET tubes. J. Sea Res. 36, 63-67.

Kranenburg, C.: The fractal structure of cohesive sediment aggregates, Estuar Coast Shelf S, 39, 451 – 460, 1994.

Kumar, R. G., Strom, K. B., and Keyvani, A. 2010: Floc properties and settling velocity of San Jacinto estuary mud under variable shear and salinity conditions, Continental Shelf Res, 30, 2067-2081.

Launay, M. 2014. Flux de matières en suspension, de mercure et de PCB particulaires dans le Rhône, du Léman à la Méditerranée. Phd thesis. 434pp.

Lee, B.J., Toorman, E. and Fettweis, M. 2014. Multimodal particle size distributions of fine-grained sediments: mathematical modeling and field investigation. Ocean Dynamics. 64, 429-441.

Lick, W., Huang H. and Jepsen R. 1993. Flocculation of fine-grained sediments due to differential settling. Journal of Geophysical Res. 98, C6, 10,279-10,288.

Mari, X., Torréton, J.P., Bich-Thuy Trinh, C., Bouvier, T., Thuoc, C.V., Lefebvre, J.-P., Ouillon, S., 2012. Aggregation dynamics along a salinity gradient in the Bach Dang estuary, North Vietnam. Estuar. Coast. Shelf Sci. 96, 151–158.

Mehta, A.H., 1989. On estuarine cohesive sediment suspension behavior. Journal of Geophysical Research, 94, C10, 14303-14314.

Mercier, B., Wendling, V., Coulaud, C., Legout, C., Gratiot, N., 2016. Développement d'un Système de Caractérisation des Agrégats et des Flocs (SCAF). c2i-2016 : 7ème Colloque Interdisciplinaire en Instrumentation. 20 21 Janvier 2016, Saint Nazaire, France, 8pp.

Pejrup, M., 1988. Flocculated suspended sediment in a micro-tidal environment. Sediment. Geol. 57, 249–256.

Pejrup, M., Edelvang, K., 1996. Measurements of in situ settling velocities in the Elbe estuary. J. Sea Res. 36, 109–113.

Pejrup, M., Mikkelsen, O.E., 2010. Factors controlling the field settling velocity of cohesive sediment in estuaries. Estuar. Coast. Shelf Sci. 87, 177–185.

Puls, W., Kuehl, H., Heymann, K., 1988. Settling velocity of mud flocs: results of field measurements in the Elbe and the Weser Estuary. In: Dronkers, J., van Leussen, W. (Eds.), Physical Processes in Estuaries. Springer-Verlag, pp. 404–424.

Ross, M.A., 1988. Vertical structure of estuarine fine sediment suspensions. Technical Report. Coastal and Oceanographic Engineering Department, University of Florida, Gainesville.

Sottolichio, A., Hurther, D., Gratiot, N., Bretel, P., 2011. Acoustic turbulence measurements of near-bed suspended sediment dynamics in highly turbid waters of a macrotidal estuary. Continental Shelf Research, 31, S36-S49.

Thorn, M.F.C., 1981. Physical processes of siltation in tidal channels. Proceedings, Hydraulic Modelling Applied to Maritime Engineering Problems, ICE, London, UK, 47–55.

Tran, D. and Strom, K., 2017. Suspended clays and silts: are they independent or dependent fractions when it comes to settling in a turbulent suspension? Continental Shelf Research, 138, 81-94.

Verney, R., Lafite, R. and Brun-Cottan, J.C. 2009. Flocculation potential of estuarine particles: the importance of environmental factors and of the spatial and seasonal variability of suspended particulate matter. Estuaries and Coasts, 32, 678-693.

Wendling, V., Gratiot, N., Legout, C., Droppo, I.G., Coulaud, C. and Mercier, B. 2015. Using an optical settling column to assess suspension characteristics within the free, flocculation and hindered settling regimes. J. of Soils and Sediment, (15) 1991-2003.

Winterwerp, J.C. 2002. On the flocculation and settling of estuarine mud. Continental shelf research, 22, 1339-1360.